

Visual-Manual Distraction Detection Using Driving Performance Indicators With Naturalistic Driving Data

Zhaojian Li, *Member, IEEE*, Shan Bao, *Member, IEEE*, Ilya V. Kolmanovsky, *Fellow, IEEE*,
and Xiang Yin, *Member, IEEE*

Abstract—This paper investigates the problem of driver distraction detection using driving performance indicators from onboard kinematic measurements. First, naturalistic driving data from the integrated vehicle-based safety system program are processed, and cabin camera data are manually inspected to determine the driver’s state (i.e., distracted or attentive). Second, existing driving performance metrics, such as steering entropy, steering wheel reversal rate, and lane offset variance, are reviewed against the processed naturalistic driving data. Furthermore, a nonlinear autoregressive exogenous (NARX) driving model is developed to predict vehicle speed based on the range (distance headway), range rate, and speed history. For each driver, the NARX model is then trained on the attentive driving data. We show that the prediction error is correlated with driver distraction. Finally, two features, steering entropy and mean absolute speed prediction error from the NARX model are selected, and a support vector machine is trained to detect driving distraction. Prediction performances are reported.

Index Terms—Distraction detection, driver modeling, nonlinear autoregressive exogenous model, steering entropy, support vector machines.

I. INTRODUCTION

DRIVER distraction is of growing concern to transportation safety. Based on a report from National Highway Traffic Safety Administration, in 2014, ten percent of fatal crashes and 18 percent of injury crashes were due to distraction [1]. From 2010 to 2014, the number of people who are injured from distraction related crashes increased from 416,000 to 431,000 [1]. Drivers can get distracted with various activities, from cell phone use, eating, to day dreaming. Recent advances in in-vehicle technologies and electronic devices place additional sources of distractions that may contribute to the increased distraction-affected accidents [2], [3]. Distraction detection and mitigation systems can play an important role in improving driving safety.

Manuscript received December 19, 2016; revised June 27, 2017 and August 14, 2017; accepted September 15, 2017. Date of publication October 19, 2017; date of current version August 1, 2018. The Associate Editor for this paper was Z. Duric. (*Corresponding author: Xiang Yin.*)

Z. Li is with the Department of Mechanical Engineering, Michigan State University, East Lansing, MI 48824 USA (e-mail: lizhaoj1@egr.msu.edu).

S. Bao is with the University of Michigan Transportation Research Institute, Ann Arbor, MI 48109 USA (e-mail: shanbao@umich.edu).

I. V. Kolmanovsky is with the Department of Aerospace Engineering, University of Michigan, Ann Arbor, MI 48109 USA (e-mail: ilya@umich.edu).

X. Yin is with the Department of Automation, Shanghai Jiao Tong University, Shanghai 200240, China (e-mail: xiangyin@umich.edu).

Color versions of one or more of the figures in this paper are available online at <http://ieeexplore.ieee.org>.

Digital Object Identifier 10.1109/TITS.2017.2754467

Depending on the activity that diverts driver’s attention, driver distraction can be categorized as visual, auditory, cognitive or visual-manual [4]. For instance, making a phone call while driving causes cognitive distraction whereas texting while driving requires multiple, concurrent resources from drivers including intense visual, manual, and cognitive engagement. While all types of driver distraction represent potential hazards for driving safety, visual-manual distraction has the most significant impact on vehicle handling since driving is a vision-intensive task while visual-manual tasks lead to frequent eye movements away from the roadway and significant performance drop in vehicle controls [5]. This paper focuses on developing algorithms to detect visual-manual distracted driving.

Current available distraction detection and mitigation systems have been prototyped using cameras or eye-tracking devices. For example, Saab’s Driver Attention System (AttenD) exploits two cameras that directly face the driver to monitor whether the driver’s gaze is within the “field relevant for driving (FRD)”. A warning will be given by vibrating the seat if the driver’s gaze is outside the FRD for two seconds. In [6], a distraction detection system is developed by measuring eye glances using an eye-tracking system. While eye movement can be a direct indication of driving distraction, accuracy and robustness of the measurements pose great challenges. Factors such as eye glasses, lighting conditions, and head rotations can disturb the tracking system. Furthermore, high-performance eye tracking systems for real on-road application are yet available and are typically prohibitively costly for mass production.

In this paper, we pursue the development of a distraction detection algorithm using kinematic signals from the vehicle Controller Area Network (CAN) bus. Exploitation of the readily available signals can avoid adding costly or obtrusive hardware. Towards this end, many steering wheel signal-based metrics have been proposed as indicators of driver distraction, from simple steering wheel standard deviation [7] to more comprehensive metrics such as steering entropy [8], [9] and high frequency steering content [10]. Longitudinal metrics, e.g., based on speed variation and distance headway variations, have also been identified as potential distraction indicators [11]–[13].

While good correlations have been reported for these approaches, their use for driver distraction detection needs further validation for the following reasons. Firstly,

in [8], [9], and [11]–[13] driver simulators are used to evaluate the proposed metrics. While state-of-the-art simulators were employed, the differences between simulated driving and naturalistic driving are not negligible. Secondly, while additional field experiments were conducted to validate the proposed metrics [7], [11]–[14], in these studies driver distraction was identified using indirect physiological measurements such as electrocardiography [7], [11]–[13] or using the prototyped distraction detection system *AttenD* [14], which inevitably introduced detection errors. Thirdly, in several existing studies secondary visual tasks were imposed to simulate distracted driving and results were compared to a base-line drive with the same drive task but without imposing distractions [7], [11]–[14]. This setup neglects the fact that chances of driver distraction are much lower when the driving task itself is demanding. Driver distractions tend to happen when the driving workload is light.

To address the above issues, in this paper, vehicle kinematic data from naturalistic driving study program [15] are used to develop driver distraction algorithm. These data have been recorded continuously on everyday driven vehicles without specified base lines. Cabin video data were captured and manually inspected to identify attentive or distracted cases; the resulting labels were used to facilitate the development and validation of the algorithms. In particular, in this paper, the afore-mentioned performance metrics are compared against the processed data. In addition, a Nonlinear Autoregressive Exogenous (NARX) model is developed for vehicle speed prediction. Based on this model, the mean of the absolute prediction error is proposed as a new metric for distraction detection. A support vector machine is then exploited for distraction detection with the identified features. Promising detection performance results are reported.

The rest of the paper is organized as follows. Section II describes the data acquisition and data processing. Performance metrics from the previous literature are reviewed and discussed in Section III. In Section IV, a NARX vehicle speed prediction model is defined and trained on attentive driving data for each subject. In Section V, support vector machines (SVMs) are trained to identify driver distractions; classification accuracy results are reported. Finally, conclusions are drawn in Section VI.

II. DATA ACQUISITION AND PROCESSING

To achieve the objectives of this study, data from the Integrated Vehicle based Safety System (IVBSS) program were used [15]. The IVBSS program was designed to support the development and testing of an integrated in-vehicle crash warning system including Forward Crash Warning, Lane Departure Warning, Lane Change/Merge Warning and Curve Speed Warning systems. Sixteen 2006 and 2007 Honda Accord vehicles were used for data collection, see Figure 1. Each vehicle was instrumented to capture information regarding the driving environment, driver activity, system behavior, and vehicle kinematics, with data collection frequency from 10 to 50 Hz.

A total of 108 randomly sampled, passenger-car drivers participated in the IVBSS study, with the sample stratified

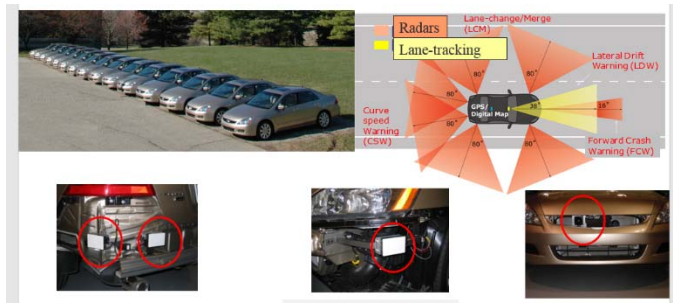


Fig. 1. Experimental vehicles used in the IVBSS program.

by age and gender. The age groups examined were younger drivers between 20 and 30 years old, middle-aged drivers between 40 and 50 years old, and older drivers between 60 and 70 years old. All drivers were required to have a valid driver's license.

Drivers used the test vehicles as their personal vehicles for a 40-day period. The first 12 days of vehicle use served as a baseline period during which warning functions were not provided to drivers, but all sensors and computations were still operating in the background and all data were recorded. The following 28 days constituted the treatment period during which functions were enabled and warnings were provided to drivers when appropriate. Only assigned participants were permitted to drive the vehicles during the test period, except for emergencies. Drivers were informed that their driving behaviors were being documented and video recorded during the whole test period and will only be used for the purpose of transportation safety research.

The cabin instrumentation in the experimental vehicles is shown in Figure 2. For this study, the data analyzed are from 16 drivers in the first 12 days of data collection, during which all warning systems were disabled. Since we need to manually inspect the cabin video frame by frame to determine the driver's state (attentive or distracted), due to limited resources we only processed datasets from 16 drivers which we believe is adequate for this study. The distracted driving episodes of interest are visual-manual tasks by the driver (e.g., texting, dialing, etc.). Cabin camera clips are manually inspected to determine the driver's status (distracted or attentive). In this study, for each driver, ten 20-second distracted episodes are identified and 50 matched control clips, in which drivers did not engage in any secondary tasks, are also identified. Kinematic signals such as steering angle, vehicle speed, and distance to the lead vehicle are recorded for the analysis and algorithm design. Note that to better analyze the correlation between the longitudinal operation and driver distraction, all clips correspond to not being in cruise control mode.

III. PERFORMANCE METRICS FOR DRIVER DISTRACTION

While a variety of driving performance metrics have been proposed for distraction detection and promising correlations have been demonstrated in previous publications, it is imperative to evaluate these metrics when applied to actual naturalistic driving data to be certain of their reference for



Fig. 2. Cabin instrumentation in the experimental vehicles including cameras and CAN signals.

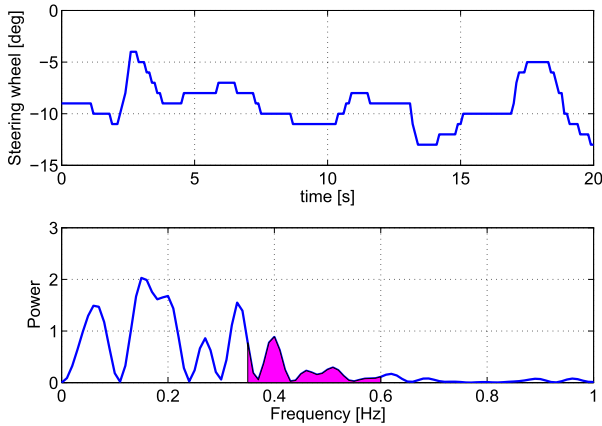


Fig. 3. High frequency steering content calculation by integrating the steering power in the 0.35-0.6 Hz frequency band. Top: steering wheel angle. Bottom: power spectrum of zero mean signal.

distraction detection. Towards this end, in this section we perform evaluations of the reported metrics using our acquired data from Section II.

A. High-Frequency Steering Content

It is reported in [10] that high frequency steering wheel (HFSW) content (in 0.35-0.6 Hz frequency band) is sensitive to both primary and secondary task loads. The computation of HFSW involves three main steps: (1) subtracting the mean from the steering signal in a time window (e.g., 20 s); (2) performing a Fourier transform to obtain the power spectrum of the resulting zero-mean steering wheel signal; and (3) integrating the steering power in the 0.35-0.6 Hz frequency band. A sample steering wheel signal trace and the power spectrum of the corresponding zero-mean signal are illustrated in Figure 3. The HFSW is then computed by integrating the power spectrum in the 0.35-0.6 Hz frequency band (magenta area in Figure 3).

The HFSW of attentive and distracted driving for the ten drivers are shown in Figure 4. The filled bars represent 25 to 75 percentile data and the horizontal red line inside each bar represents the medium. The red “+”s are data classified

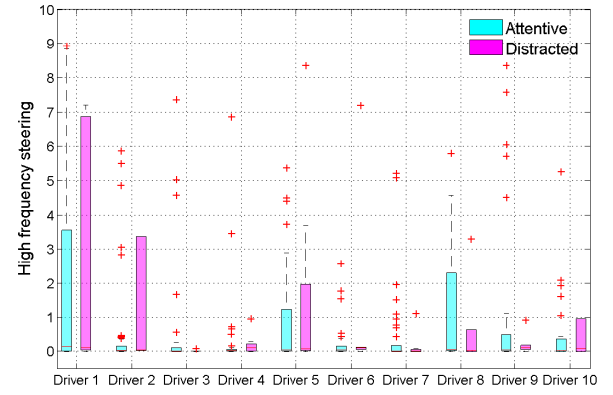


Fig. 4. Box plots of high frequency steering wheel for attentive and distracted driving comparisons.

as outliers. From Figure 4 we see that the magnitude of HFSW varies significantly between individual drivers. This may be due to the fact that some drivers tend to move the steering wheel more frequently than others. Also, the reported correlation between higher HFSW and driver distraction [10] is not consistently implied among the drivers. For Drivers 3, 7, 8 and 9, HFSW is lower when the driver is distracted, which indicates that HFSW may not be a good universal metric for distraction detection.

B. Steering Entropy

Steering entropy is an indication of steering smoothness and predicability. The rationale for using it is that attentive drivers continuously assess the environment and unconsciously apply smooth and predictable steering control. On the other hand, distracted drivers tend to introduce large maneuvers for error correction, leading to decreased predicability.

Steering entropy is proposed in [8] to quantify the steering predicability. As illustrated in Figure 5, at each time stamp t , a second-order Taylor expansion is exploited to predict the steer $\theta_p(t)$ based on previous samples of the steering wheel angle, θ , as follows:

$$\begin{aligned} \theta_p(t) = & \theta(t-1) + (\theta(t-1) - \theta(t-2)) \\ & + \frac{1}{2}((\theta(t-1) - \theta(t-2)) - (\theta(t-2) - \theta(t-3))), \end{aligned} \quad (1)$$

which can be simplified as

$$\theta_p(t) = \frac{5}{2}\theta(t-1) - 2\theta(t-2) + \frac{1}{2}\theta(t-3). \quad (2)$$

The prediction error $e(t)$ is then calculated as the difference between the actual value $\theta(t)$ and the predicted value $\theta_p(t)$ from Equation (2):

$$e(t) = \theta(t) - \theta_p(t). \quad (3)$$

It is recommended in [8] that the prediction period should be shorter than 150 ms, which corresponds to the lowest frequency that can be used to represent a human driver's control response in manual tracking tasks. In this study,

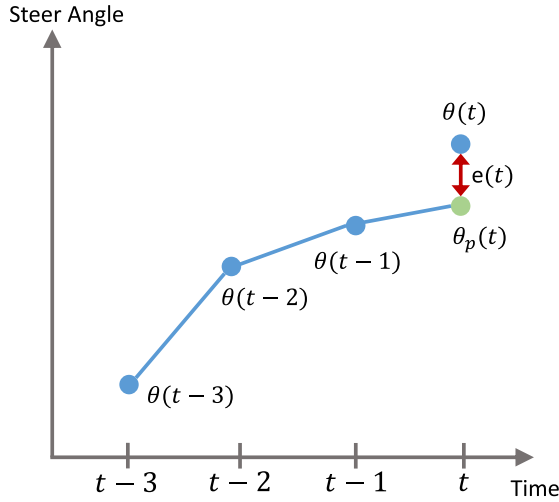


Fig. 5. Steering wheel prediction.

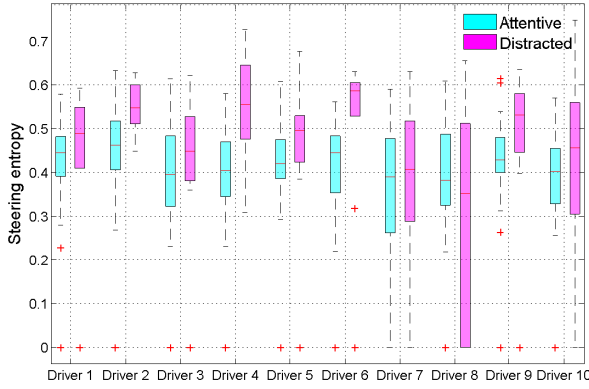


Fig. 6. Box plots of steering entropy for attentive and distracted driving comparisons.

the prediction period is chosen to be the sampling time used in the data, i.e., 100 ms.

The error distribution in a time window (e.g., a 10 sec window) can then be computed and the value α such that 90% error falls in the $[-\alpha, \alpha]$ interval can be calculated. The error distribution is then divided into nine bins based on α (see [8] for details). The steering entropy H_p is calculated as

$$H_p = \sum_{i=1}^9 -p_i \log_9 p_i, \quad (4)$$

where p_i represents the proportion of error data that falls into the i th bin.

We compute the steering entropy on the collected naturalistic driving data and show comparisons between attentive and distracted driving for the 10 drivers in Figure 6.

A clear correlation between high steering entropy and driver distraction can be seen in Figure 6 for all drivers except for Driver 8 which shows comparable results. These comparisons show that steering entropy can be a good metric for online distraction detection. We thus use steering entropy as one of the features for online distraction detection in Section V

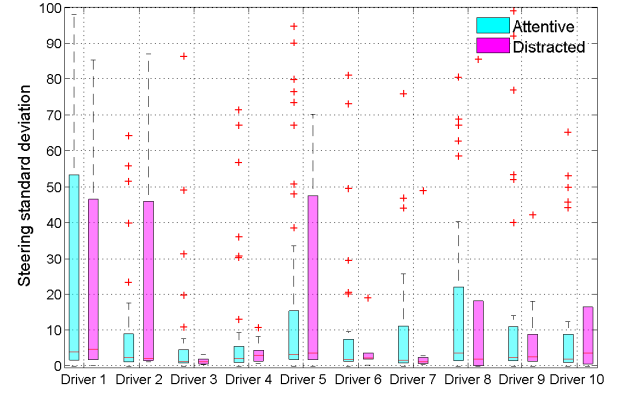


Fig. 7. Box plots of steering standard deviation for attentive and distracted driving comparisons.

C. Steering Wheel Standard Deviation

As a quantification of steering variation, steering wheel standard deviation is proposed by Liu and Lee as a metric for distraction detection [7]. In a time window with N steering samples, the steering wheel standard deviation, σ , is computed as $\sigma = \sqrt{\sum_{i=1}^N (\theta(i) - \bar{\theta})^2}$ with $\bar{\theta} = \frac{1}{N} \sum_{i=1}^N \theta(i)$ being the steering mean. In this subsection, we check the proposition using the collected naturalistic driving data. The comparisons between distracted and attentive driving for the ten drivers are shown in Figure 7.

We observe from Figure 7 that the correlation between driver distraction and higher steering standard deviation exists for Drivers 2, 5, and 10. At the same time, the other seven drivers show the opposite correlation. Therefore, we do not use this metric as a feature for distraction detection.

D. Speed Variations and Distance Headway Variations

Longitudinal metrics such as speed variations and distance headway variations have also been proposed as driving distraction indicators [11]–[13]. The rationale is that attentive drivers tend to produce less jerks while distractions can cause large corrective maneuvers.

The standard deviations of vehicle speed and distance headway based on the naturalistic driving data are illustrated in Figures 8 and 9, respectively. It appears that for most of the drivers the reported correlations between higher speed or distance headway variations and driver distraction are not reflected in the collected naturalistic driving data. The reason for this may be that speed and distance headway are highly dependent on the driving environment. In the next section, in an attempt to improve the correlation, we develop a driver model by considering the distance headway and vehicle speed jointly.

As demonstrated in Figures 6-9, clear correlations can be found between high steering entropy and driving distraction across the drivers while no clear correlations between driving distraction and other factors are found. Furthermore, the steering entropy varies significantly across the drivers. To robustly use this metric for prediction, we use driver-dependent scaling

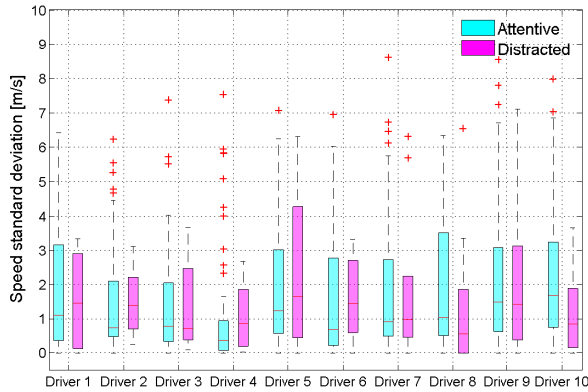


Fig. 8. Box plots of vehicle speed standard deviation for comparing attentive and distracted driving.

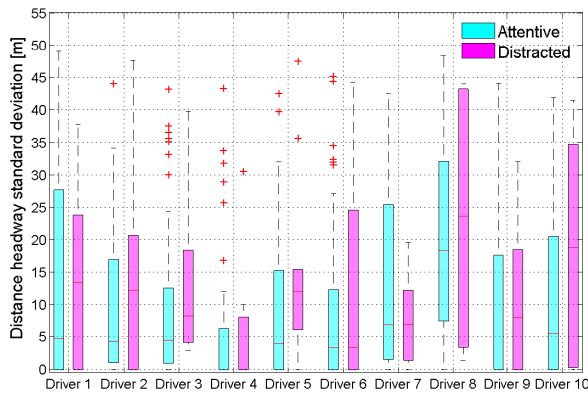


Fig. 9. Box plots of distance headway standard deviation for comparing attentive and distracted driving.

factors (i.e., minimum and maximum) to scale the steering entropy between 0 and 1.

IV. NARX SPEED PREDICTION MODELING

In Section III-D, preliminary longitudinal metrics such as standard deviation of vehicle speed and standard deviation of distance headway proposed in [11]–[13] are shown to be lacking as distraction indicators. We hypothesize that this happens for the reason that longitudinal metrics may highly depend on driving environment, e.g., traffic density and lead vehicle dynamics. For example, following an aggressive driver in a congested traffic flow can produce a fair amount of jerks even when the driver is attentive. Furthermore, distance headway and vehicle speed could be considered together to improve the correlation.

In the sequel, we develop a driver model that considers both the speed-distance correlation and driving dynamics. While physics-based models such as Optimal Velocity Model (OVM) [16]–[19] are available, certain parameters need to be tuned for each driver. In this paper, we pursue a data-driven approach since the driving data are readily available to avoid the tunings. The schematic diagram of the proposed model is shown in Figure 10. The driver reacts to the range (distance to lead vehicle, denoted by d), range

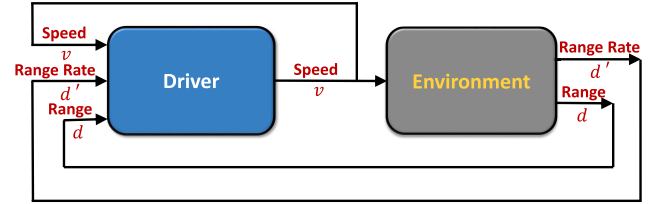


Fig. 10. Schematic diagram of the proposed driver model for vehicle speed control. At each time step, the driver perceives current vehicle speed, evaluates the vehicle’s range and range rate from the vehicle ahead, and then adjusts its speed using gas/brake pedal. The range and range rate will be updated at next time step through interaction with the vehicle ahead.

rate (distance change rate to lead vehicle, denoted by d') and ego vehicle speed (denoted by v), and then applies the gas or brake pedal to adjust the speed. The vehicle then interacts with the environment, updating the range and range rate which closes the system loop. Note that the model considers both the driving dynamics (reflected in range and range rate) and range-speed correlations.

The driver model can be used to emulate the driver’s reaction and predict vehicle speed based on the near history of range, range rate and vehicle speed. We hypothesize that the prediction error for distracted driving would be larger than that of normal driving since distracted driving is more “unpredictable”. It is noted that different drivers may have different sense of “safe” distance, potentially requiring in different driver models. Therefore, the driver model is customized for each driver.

In this paper, we use a Nonlinear Autoregressive Exogenous (NARX) model [20]–[22] to represent the driver’s speed control:

$$Y(t) = f(Y(t-1), \dots, Y(t-N_y), U(t-1), U(t-N_u)), \quad (5)$$

where $Y(t)$ represents the output of the model and $Y(t) = v(t)$ represents the vehicle speed; $U(t) = \{d(t), d'(t)\}$ represents the input vector including range and range rate. The parameters N_u and N_y are the input delay and output delay, respectively.

We employ an Artificial Neural Network (ANN) as the function approximator for the NARX model in Equation (5). The model is trained for each driver on the attentive driving data set. The size of hidden neurons in the ANN is chosen as ten based on five-fold cross validation. Specifically, we randomly partition the training data into five sets. We then run five training runs and for each run one of the five sets is used to test the prediction performance and the rest four sets are used for ANN training. The prediction errors are then averaged over the five runs. We tried different combinations of parameters N_y and N_u and picked ten as the hidden size since no clear improvements are found with more neurons. The N_y and N_u are parameters that are related to driver’s response time. The driver’s response time are typically around 0.45-1 second [18], [19]. We tune these two parameters also based on the average prediction error of the five-fold cross-validation illustrated in Figure 11. The parameters are chosen as $N_y = 1$ and $N_u = 5$ to balance small error and required buffer size.

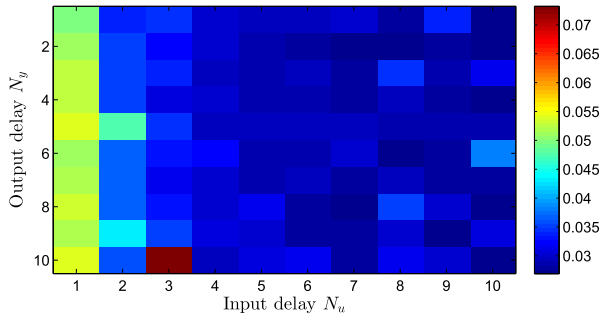


Fig. 11. Distribution of five-fold cross-validation prediction error over parameters N_y and N_u .

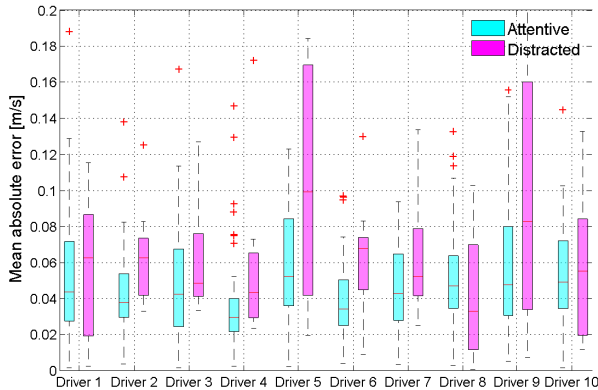


Fig. 12. Box plots of mean absolute ANN prediction error for attentive and distracted driving comparisons.

For each driver, we train its driving model using 60% of the attentive driving data and the rest 40% are used for testing. The mean absolute prediction error box plots for the ten drivers are illustrated in Figure 12 with distracted and attentive drives plotted side by side. It can be seen that the model is able to predict the vehicle speed accurately for attentive driving (less than 0.1 m/s). Furthermore, distracted driving cases clearly yield higher prediction errors than attentive driving cases for all drivers except Driver 8, which has similar prediction error for distracted and attentive driving. Nonetheless, the prediction error generated from the NARX model (5) appears to be a good distraction indicator. We next exploit machine learning techniques for distraction detection.

Remark 1: In this paper, we train separate ANN-based NARX models for different drivers since drivers tend to have very different driving behaviors as demonstrated in Figures 6-9 and Figure 12. For practical implementations, the training data can be obtained by sampling, that is, we randomly sample the driver's driving data for a fixed time window through, for example, vehicle-to-cloud communication or onboard storage. Since distracted driving is generally much less frequent than attentive driving, with an appropriate sampling size, the sampled data is representative of the driver's attentive driving. This sampling strategy will be considered in our future work. With the trained model, the distraction prediction system can start functioning.

V. SVM DISTRACTION DETECTION

In Section III and Section IV, we identified metrics such as steering entropy and speed prediction error from the NARX

driving model as feasible distraction indicators. In this section, we exploit machine learning algorithms that can be implemented in real-time for distraction detection. Specifically, we use a support vector machine (SVM) to classify distracted and attentive driving.

Given a set of N data points $x_i \in \mathbb{R}^n$, $i = 1, \dots, N$ and associated binary class labels $y_i \in \{-1, +1\}$, $i = 1, \dots, N$, a standard classification problem is to find a mapping function $f(x)$ to accurately separate the two classes. The Support Vector Machine (SVM) is based on supervised learning that has been successfully used for many applications including in the field of pattern recognition [23], [24], financial engineering [25]–[27], and automotive engineering [28]–[30]. SVM advantages over alternative techniques include substantial theory foundation, effective computational algorithms known to yield global optima, and good generalization ability [29]. In SVM training, two parameters γ and C are typically tuned through cross-validation where $\gamma > 0$ controls the generalization ability of the SVM classifier and $C > 0$ is a positive scaler to penalize the constraint violations. More technical details on SVM can be referred to [29], [31], and references therein.

We use the SVM to classify distracted and attentive driving based on the identified features, i.e., steering entropy and mean absolute speed prediction error from the NARX model we developed in Section IV. For each driver, we train an SVM over the processed driving data (the two features and manually examined driving status, i.e., attentive or distracted) for about 60 episodes. Note that the kernel scaling factor γ and constraint violation penalty weight C need to be specified before the SVM training. We run the ten-fold cross-validation procedure to determine an optimal γ and C . Specifically, we vary γ and C in a large range and for each (γ, C) pair we randomly partition the data into ten sets. We then run ten training runs and for each run one of the ten sets is reserved to test the SVM prediction performance and the rest nine sets are used for SVM training. The classification accuracy, averaged over the ten runs, is referred to as the ten-fold cross-validation accuracy.

The contour plot of the ten-fold cross-validation accuracy in the $\log(\gamma) - \log(C)$ plane for Driver 6 is illustrated in Figure 13. The best cross-validation accuracy is 93.8% and can be obtained by choosing $C = 1$ and $\gamma = 0.01$. The same tuning process is used for all other drivers to select γ and C for the SVM training.

With tuned γ and C , we train the SVM over the data of Drivers 1-10 and we test the SVM prediction using the data from Drivers 11-16. The prediction performance of testing for the six drivers are illustrated in Table I. The term *True positive* means the number of correctly identified distraction cases while *True negative* represents the number of correctly identified attentive cases. On the other hand, *False negative* and *False positive* represent, respectively, the number of missed detection of distraction and the number of attentive driving cases that are incorrectly classified as distracted.

As we can observe from Table I, the overall accuracy across all drivers can be as high as around 95%. Specifically, the *False positive* cases are very few; only Driver 14 has one attentive

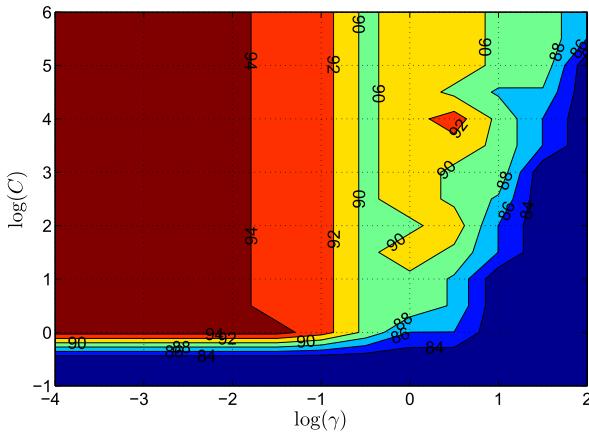


Fig. 13. Cross-validation accuracy of SVM classification as a function of γ and C for Driver 6.

TABLE I
DISTRACTION DETECTION PERFORMANCE WITH THE SVMs

	Total cases	TP	TN	FN	FP	Accuracy (%)
Driver 11	60	9	50	1	0	98.33
Driver 12	59	8	49	2	0	96.61
Driver 13	58	7	48	3	0	94.83
Driver 14	60	7	50	3	1	93.3
Driver 15	60	8	50	2	0	96.67
Driver 16	60	8	50	2	0	96.67

driving case that is mislabeled as distracted driving. On the other hand, the average false negative rate, defined as $\frac{FN}{FN+TN}$, is 78.3% over all drivers; this is a promising initial result which can be further improved on. Future work will include exploiting Recurrent Neural Networks [32] to improve the detection performance.

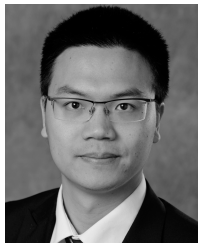
VI. CONCLUSIONS

In this paper, we processed naturalistic driving data from the Integrated Vehicle Based Safety System (IVBSS) program and manually inspected the cabin camera data to determine the driver's state (i.e., distracted or attentive). Based on the data, we reviewed existing performance metrics for driver distraction and showed good correlation between driver distraction and steering entropy, whereas the correlation is lacking for other metrics. Furthermore, we developed a Nonlinear Autoregressive Exogenous (NARX) driving model to predict vehicle speed based on range, range rate, and speed history. An artificial neural network was used as the function approximator and trained with attentive driving data. We demonstrated that driver distraction yields higher prediction error than attentive driving. Finally, we used steering entropy and the absolute mean of speed prediction error as features to develop a support vector machine for driver distraction detection. The SVM approach is capable of achieving a high overall accuracy of 95% and a false positive rate about 78.3% when trained on individual driver specific data.

REFERENCES

- [1] T. S. Facts, "Distracted driving 2013," Nat. Highway Traffic Safety Admin., Washington, DC, USA, Tech. Rep. DOT HS 812 132, Apr. 2015.
- [2] M. Hoedemaeker and M. Neerinx, "Attuning in-car user interfaces to the momentary cognitive load," in *Foundations of Augmented Cognition*. Berlin, Germany: Springer, 2007, pp. 286–293. [Online]. Available: http://dx.doi.org/10.1007/978-3-540-73216-7_32
- [3] Y. Liao, S. E. Li, W. Wang, Y. Wang, G. Li, and B. Cheng, "Detection of driver cognitive distraction: A comparison study of stop-controlled intersection and speed-limited highway," *IEEE Trans. Intell. Transp. Syst.*, vol. 17, no. 6, pp. 1628–1637, Jun. 2016.
- [4] K. Sprattler, "Distracted driving: What research shows and what states can do," Governor's Highway Safety Assoc., Washington, DC, USA, Tech. Rep., 2001. [Online]. Available: http://sha2.aladata.com/articles/GHSA_distracted_driving_FullRpt-7Jul11.pdf
- [5] S. Bao, Z. Guo, C. Flannagan, J. Sullivan, J. R. Sayer, and D. LeBlanc, "Distracted driving performance measures spectral power analysis," *Transp. Res. Rec., J. Transp. Res. Board*, vol. 2518, pp. 68–72, Dec. 2015.
- [6] H. Zhang, M. R. H. Smith, and G. J. Witt, "Identification of real-time diagnostic measures of visual distraction with an automatic eye-tracking system," *Hum. Factors*, vol. 48, no. 4, pp. 805–821, 2006.
- [7] B.-S. Liu and Y.-H. Lee, "In-vehicle workload assessment: Effects of traffic situations and cellular telephone use," *J. Saf. Res.*, vol. 37, no. 1, pp. 99–105, 2006.
- [8] O. Nakayama, T. Futami, T. Nakamura, and E. R. Boer, "Development of a steering entropy method for evaluating driver workload," SAE Tech. Paper 1999-01-0892, 1999.
- [9] E. R. Boer, M. E. Rakauskas, N. J. Ward, and M. A. Goodrich, "Steering entropy revisited," in *Proc. 3rd Int. Driving Symp. Hum. Factors Driver Assessment, Training, Vehicle Design*, 2005, pp. 25–32.
- [10] J. R. Mclean and E. R. Hoffmann, "Analysis of drivers' control movements," *Hum. Factors*, vol. 13, no. 5, pp. 407–418, 1971.
- [11] J. Engström, E. Johansson, and J. Östlund, "Effects of visual and cognitive load in real and simulated motorway driving," *Transp. Res. F, Traffic Psychol. Behav.*, vol. 8, no. 2, pp. 97–120, 2005.
- [12] O. Carsten and K. Brookhuis, "The relationship between distraction and driving performance: Towards a test regime for in-vehicle information systems," *Transp. Res. F, Traffic Psychol. Behaviour*, vol. 8, no. 2, pp. 75–77, 2005.
- [13] J. Östlund *et al.*, "Driving performance assessment—methods and metrics," Adaptive Integrated Driver-Vehicle Interface, Gothenburg, Sweden, Tech. Rep. IST-1-507674-IP, 2005.
- [14] K. Kircher and C. Ahlstrom, "Predicting visual distraction using driving performance data," *Ann. Adv. Autom. Med.*, vol. 54, pp. 333–342, Jan. 2010.
- [15] J. Sayer *et al.*, "Integrated vehicle-based safety systems field operational test final program report," Univ. Michigan Transp. Res. Inst., Ann Arbor, MI, USA, Tech. Rep. UMTRI-2010-36, 2011.
- [16] N. I. Li, C. R. He, and G. Orosz, "Sequential parametric optimization for connected cruise control with application to fuel economy optimization," in *Proc. 55th IEEE Conf. Decision Control*, Dec. 2016, pp. 227–232.
- [17] N. I. Li and G. Orosz, "Dynamics of heterogeneous connected vehicle systems," *IFAC-PapersOnLine*, vol. 49, no. 10, pp. 171–176, 2016. [Online]. Available: <http://www.sciencedirect.com/science/article/pii/S2405896316307340>
- [18] G. Orosz, "Connected cruise control: Modelling, delay effects, and nonlinear behaviour," *Vehicle Syst. Dyn.*, vol. 54, no. 8, pp. 1147–1176, 2016.
- [19] G. Orosz, R. E. Wilson, and G. Stépán, "Traffic jams: Dynamics and control," *Philos. Trans. Roy. Soc. London A, Math. Phys. Sci.*, vol. 368, no. 1928, pp. 4455–4479, 2010. [Online]. Available: <http://rsta.royalsocietypublishing.org/content/368/1928/4455>
- [20] H. M. Zarate-Solano and D. R. Zapata-Sanabria, "Clustering and forecasting inflation expectations using the world economic survey: The case of the 2014 oil price shock on inflation targeting countries," Banco Republica, Bogotá, Colombia, Tech. Rep. 993, 2017.
- [21] D. Sayfeddine, "Nonlinear autoregressive neural network with exogenous inputs based solution for local minimum problem of agent tracking using quadrotor," *Electron. Sci. J., Eng. J. Don*, vol. 29, no. 2, 2014. [Online]. Available: <http://www.ivdon.ru/en/magazine/archive/n2y2014/2355>
- [22] G. Mustafaraj, J. Chen, and G. Lowry, "Thermal behaviour prediction utilizing artificial neural networks for an open office," *Appl. Math. Model.*, vol. 34, no. 11, pp. 3216–3230, 2010.

- [23] H. Drucker, D. Wu, and V. N. Vapnik, "Support vector machines for spam categorization," *IEEE Trans. Neural Netw.*, vol. 10, no. 5, pp. 1048–1054, Sep. 1999.
- [24] S. Hua and Z. Sun, "A novel method of protein secondary structure prediction with high segment overlap measure: Support vector machine approach," *J. Mol. Biol.*, vol. 308, no. 2, pp. 397–407, 2001.
- [25] T. V. Gestel *et al.*, "Financial time series prediction using least squares support vector machines within the evidence framework," *IEEE Trans. Neural Netw.*, vol. 12, no. 4, pp. 809–821, Jul. 2001.
- [26] F. E. H. Tay and L. Cao, "Application of support vector machines in financial time series forecasting," *Omega*, vol. 29, no. 4, pp. 309–317, 2001.
- [27] K.-J. Kim, "Financial time series forecasting using support vector machines," *Neurocomputing*, vol. 55, no. 1, pp. 307–319, 2003.
- [28] W.-C. Hong and P.-F. Pai, "Predicting engine reliability by support vector machines," *Int. J. Adv. Manuf. Technol.*, vol. 28, nos. 1–2, pp. 154–161, 2006. [Online]. Available: <http://dx.doi.org/10.1007/s00170-004-2340-z>
- [29] I. V. Kolmanovsky and E. G. Gilbert, "Support vector machine-based determination of gasoline direct injected engine admissible operating envelope," SAE Tech. Paper 2002-01-1301, 2002. [Online]. Available: <http://dx.doi.org/10.4271/2002-01-1301>
- [30] S.-H. Chen, J.-S. Pan, and K. Lu, "Driving behavior analysis based on vehicle OBD information and AdaBoost algorithms," in *Proc. Int. MultiConf. Eng. Comput. Sci.*, vol. 1. 2015, pp. 18–20.
- [31] N. Cristianini and J. Shawe-Taylor, *An Introduction to Support Vector Machines and Other Kernel-Based Learning Methods*. New York, NY, USA: Cambridge Univ. Press, 2000.
- [32] L. Bontemps, V. L. Cao, J. McDermott, and N.-A. Le-Khac, "Collective anomaly detection based on long short term memory recurrent neural network," *CoRR*, Mar. 2017. [Online]. Available: <http://arxiv.org/abs/1703.09752>



Zhaojian Li (S'15–M'16) received the B.S. degree in civil aviation from the Nanjing University of Aeronautics and Astronautics, Nanjing, China, in 2010, and the M.S. and Ph.D. degrees from the Department of Aerospace Engineering, University of Michigan, Ann Arbor, MI, USA, in 2014 and 2016, respectively. From 2010 to 2012, he was an Air Traffic Controller with the Shanghai Area Control Center, Shanghai, China. From 2014 to 2015, he was an Intern with Ford Motor Company, Dearborn, MI, USA. He is currently an Assistant Professor

with the Department of Mechanical Engineering, Michigan State University. His current research interests include optimal control, autonomous vehicles, and intelligent transportation systems. He was a recipient of the National Scholarship from China.



Shan Bao is currently an Associate Research Scientist with the Human Factors Group, University of Michigan Transportation Research Institute, where she has been conducting research on human factors and driver distraction, driver-behavior modeling, large-scale data analysis, driver training for automated vehicles, and the evaluation of advanced in-vehicle safety systems since 2009.

She received the Ph.D. degree in mechanical and industrial engineering from The University of Iowa in 2009. She has led and conducted multiple, large, simulator and naturalistic-driving studies for industry and government sponsors. Her areas of expertise include the statistical analysis of crash data sets and naturalistic data, experimental design, algorithm development to identify driver states, evaluation of driving-safety technologies, measurement of driver performance, driver decision making, and statistical and stochastic modeling techniques. She currently serves as the Chair of the Surface Transportation Technical Group, Human Factors and Ergonomics Society.



Ilya V. Kolmanovsky (F'08) received the M.S. and Ph.D. degrees in aerospace engineering from the University of Michigan, Ann Arbor, MI, USA, in 1993 and 1995, respectively, and the M.A. degree in mathematics from the University of Michigan in 1995.

He is currently a Full Professor with the Department of Aerospace Engineering, University of Michigan. His current research interests include control theory for systems with state and control constraints, and control applications to aerospace

and automotive systems.

He was with Ford Research and Advanced Engineering, Dearborn, MI, USA, for 15 years. He is named as an Inventor on 92 U.S. patents. He was a recipient of the Donald P. Eckman Award of the American Automatic Control Council.



Xiang Yin (S'14–M'17) was born in Anhui, China, in 1991. He received the B.Eng. degree from Zhejiang University in 2012, and the M.S. and Ph.D. degrees from the University of Michigan, Ann Arbor, in 2013 and 2017, respectively, all in electrical engineering. He is currently with the Department of Automation, Shanghai Jiao Tong University. His research interests include supervisory control of discrete-event systems, model-based fault diagnosis, formal methods, and security and their applications to cyber and cyberphysical systems.

Dr. Yin received the Outstanding Reviewer Award from AUTOMATICA in 2016, the Outstanding Reviewer Award from the IEEE TRANSACTIONS ON AUTOMATIC CONTROL in 2017, and the IEEE Conference on Decision and Control Best Student Paper Award Finalist in 2016. He is a Co-Chair of the IEEE CSS Technical Committee on Discrete Event Systems.